Journal of Sound and Vibration 330 (2011) 1977–1984

Contents lists available at ScienceDirect

Journal of Sound and Vibration

journal homepage: www.elsevier.com/locate/jsvi

A new measure of efficiency for model reduction: Application to a vibroimpact system

T.G. Ritto [a,*], F.S. Buezas [b], Rubens Sampaio [c]

[a] Department of Mechanical Engineering (PGMEC), Universidade Federal Fluminense, Rua Passo da Patria 156, Boa Viagem, 24210-240, Niteroi, RJ, Brazil
[b] Department of Physics, Universidad Nacional del Sur, Av Alem, 1253, Bahía Blanca, CONICET, Argentina
[c] Department of Mechanical Engineering, PUC-Rio, Rua Marquês de São Vicente, 225, Gávea, 22453-900, RJ, Brazil

ARTICLE INFO

Article history:
Received 14 June 2010
Received in revised form
26 October 2010
Accepted 2 November 2010
Handling Editor: H. Ouyang
Available online 19 November 2010

ABSTRACT

The aim of this paper is to propose a new way to measure the efficiency of the proper orthogonal decomposition (POD) to construct a reduced-order model in Structural Dynamics. It investigates the efficiency of three reduced-order models for a vibroimpact problem: (1) POD_{dir}-basis, which is the basis constructed using the direct method of the proper orthogonal decomposition; (2) POD_{snap}-basis, which is the basis constructed using the snapshot method of the POD; and (3) LIN-basis, which is the basis composed by the normal modes of the associated linear (LIN) conservative system. The efficiency is measured in terms of (1) number of elements to represent the dynamics with a given precision and (2) computational cost to simulate the time response within a given precision.

1. Introduction

In this paper we deal with a problem of infinite-dimension and we want to construct appropriate finite dimension subspaces to capture the essential features of the dynamics, in the following when we use the word *basis* it refers to the basis of the approximation subspace. The strategy is to fix the error of the approximation and to look for bases that will give approximations of the solution within the error previously fixed.

The proper orthogonal decomposition (POD), also called Karhunen–Loève decomposition (KLD) [1,2], is increasingly used to construct reduced-order models in Structural Dynamics [3–6]. It is able to capture the coherent structures of a linear or nonlinear dynamics, and the POD-basis is the best basis in the sense that if one fixes the dimension of approximation subspace it gives the minimal error, considering all subspaces of same dimension, to represent the dynamical response of a mechanical system [1,2]. Note that this condition of optimality does not assure that the reduced-order model constructed with the POD-basis will run the simulation (time integration) faster than another reduced-order model. It is only assured that the error, among all the subspaces of same dimension, will be the smallest. This is a point that is not usually remarked and will be further depicted in this paper.

For linear dynamical systems, the normal modes of the associated linear (LIN) conservative system have information about the dynamics; LIN-basis is the basis generated by a set of normal modes. It should be noticed that the approximation can be very inefficient if the wrong modes are chosen. The modes that are important for the dynamics in analysis should be carefully chosen, so that the LIN-basis can be efficient. For nonlinear dynamical systems the LIN-basis computed from some linearization might not be so effective.

* Corresponding author.
E-mail addresses: thiagoritto@gmail.com (T.G. Ritto), fbuezas@gmail.com (F.S. Buezas), rsampaio@puc-rio.br (R. Sampaio).

0022-460X
doi:10.1016/j.jsv.2010.11.004

On the other hand, POD-basis is able to capture, in a compact form, most of the phenomenon of interest (linear or nonlinear dynamics, for example). One characteristic of the POD-basis is its sensitivity to load conditions. In other words, if the POD-basis is computed for a given level of excitation in a nonlinear problem, and then it is used to represent the dynamics of the same system for a higher level of excitation, probably the results will not be satisfactory since the characteristics of the dynamics change.

There are few works that compare the efficiency between LIN-basis and POD-basis for nonlinear dynamical systems [7,8]. In none of these works the analysis took into account the time needed to perform the time-integration procedure. In [7] a comparison among LIN-basis, Lanczos-basis, and POD-basis is made for the nonlinear dynamics of a wind turbine; POD-basis has performed better. In [8] it has been shown that POD-basis and LIN-basis present similar results, for the six nonlinear problems analyzed. To focus the attention on the results of the reduced-order models, a very simple mechanical system is considered in the numerical analysis. Nevertheless, this system has impacts, which induces local discontinuities. An analysis of model reduction using POD-basis for the dynamics of a vibroimpact system is done in [9,10].

This paper is organized as follows. The model obtained using the finite element method is presented in Section 2, then, in Section 3, the reduced-order models are introduced. The convergence criterion is given in Section 4, and the numerical results are discussed in Section 5. Finally, the concluding remarks are made in Section 6.

2. Finite element approximation

Consider the system of a bar with axial displacement field, u, sketched in Fig. 1.

The dynamics of the bar used in the analysis is given by the following equation:

$$\rho A\frac{\partial^2 u(x,t)}{\partial t^2}+c_1\frac{\partial u(x,t)}{\partial t}+c_2\frac{\partial^3 u(x,t)}{\partial t\partial x^2}-EA\frac{\partial^2 u(x,t)}{\partial x^2} = \delta(x-L)f(t)+\delta(x-L)f_{\text{imp}}(u(L,t)), \tag{1}$$

with boundary conditions $u(x,t)|_{x=0}=0$ and $EA\partial u(x,t)/\partial x|_{x=L}=0$ (the bar is fixed at x=0 and free at x=L). Where A is the cross-sectional area, E is the elasticity modulus, ρ is the density, c_1 and c_2 are the damping coefficients, f is the applied force per unit length, and f_{imp} is the impact force. The Dirac-delta function $\delta(x-L)$, for our propose here, can be defined as being equal to zero everywhere except at x=L and is constrained to satisfy $\int_0^L \delta(x-L)=1$; a rigorous definition needs distribution theory. The external forces are applied on the boundary x=L and are written as

$$f(t)=A_f\sin(2\pi\omega_f t), \tag{2}$$

where A_f is the amplitude of the excitation force, ω_f is the excitation frequency (in Hertz). And

$$f_{\text{imp}}(u(L,t))=-\gamma[k(u(L,t)-\text{gap})]\begin{cases}\gamma=0 & \text{if } u(L,t)<\text{gap},\\ \gamma=1 & \text{if } u(L,t)>\text{gap},\end{cases} \tag{3}$$

where k is the stiffness related to the obstacle and gap is the distance from the bar to the obstacle.

Eq. (1) is discretized by means of the finite element method [11]. The elemental displacement field is written as $u^{(e)}(\xi,t)=\mathbf{N}(\xi)\mathbf{u}^{(e)}(t)$, where the linear shape functions used are $\mathbf{N}(\xi)=[(1-\xi)/2\ (1+\xi)/2]$, $-1\le\xi\le 1$, and the elemental displacements are $\mathbf{u}^{(e)}(t)=[\mathbf{u}_1^{(e)}(t)\ \mathbf{u}_2^{(e)}(t)]^T$. The final discretized system, after matrix assembling, is the following:

$$\mathbf{M}\ddot{\mathbf{u}}(t)+\mathbf{C}\dot{\mathbf{u}}(t)+\mathbf{K}\mathbf{u}(t)=\mathbf{f}(t)+\mathbf{f}_{\text{imp}}(\mathbf{u}(t)), \tag{4}$$

with zero initial conditions, $\mathbf{u}_0$=$\mathbf{0}$ and $\mathbf{v}_0$=$\mathbf{0}$, where $\mathbf{M}$, $\mathbf{C}$, and $\mathbf{K}$ are the mass, proportional damping, and stiffness matrices, $\mathbf{u}$ is the response of the system, $\mathbf{f}$ is the excitation force, and $\mathbf{f}_{\text{imp}}$ is the impact force. A distinction should be made between $u(x,t)$ and $\mathbf{u}(t)$. The displacement field $u:[0,L]\times[0,T]\to\mathbb{R}$ is the solution of the continuous problem and the displacement vector $\mathbf{u}(t)\in\mathbb{R}^m$ contains the values of the displacements at the nodes of the mesh.

A proportional damping is used, i.e., the damping matrix is written as a linear combination of the mass and the stiffness matrices, $\mathbf{C}=\alpha\mathbf{M}+\beta\mathbf{K}$, where α and β are positive constants. These constants can be deduced by observing Eq. (1), $\alpha=c_1/(\rho A)$ and $\beta=c_2/(EA)$, in which c_1 and c_2 are the damping coefficients, both positive.

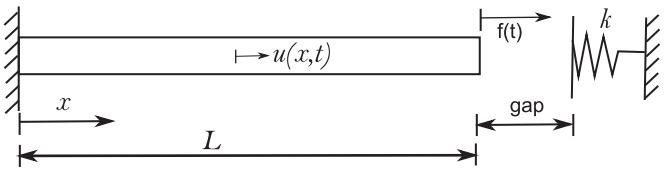

Fig. 1. Scheme of a bar impacting an obstacle.

3. Reduced-order models

The matrices $\mathbf{M}$, $\mathbf{C}$, and $\mathbf{K}$ of Eq. (4) are in $\mathbb{R}^{m\times m}$. To construct the reduced-order model, let $\mathbf{\Phi}$ in $\mathbb{R}^{m\times n}$ $(n<m)$, which has columns formed by independent vectors, the basis of the approximation subspace. Taking the approximation $\mathbf{u}(t)=\mathbf{\Phi q}(t)$ and projecting the equations in the subspace generated by the columns of $\mathbf{\Phi}$, the reduced-order system is written as

$$\mathbf{M}_r\ddot{\mathbf{q}}(t)+\mathbf{C}_r\dot{\mathbf{q}}(t)+\mathbf{K}_r\mathbf{q}(t)=\mathbf{\Phi}^{\mathrm{T}}[\mathbf{f}(t)+\mathbf{f}_{\mathrm{imp}}(\mathbf{\Phi q}(t))], \tag{5}$$

with initial conditions $\mathbf{q}_0=\mathbf{0}$ and $\boldsymbol{v}_0=\mathbf{0}$, where the reduced matrices are given by

$$\mathbf{M}_r=\mathbf{\Phi}^{\mathrm{T}}\mathbf{M}\mathbf{\Phi},\quad \mathbf{C}_r=\mathbf{\Phi}^{\mathrm{T}}\mathbf{C}\mathbf{\Phi},\quad \mathbf{K}_r=\mathbf{\Phi}^{\mathrm{T}}\mathbf{K}\mathbf{\Phi}, \tag{6}$$

and $\mathbf{q}$ is the reduced-order system response.

Three different reduction bases are used in the analysis as columns of $\mathbf{\Phi}$. The first one is the LIN-basis, which is composed by the chosen normal modes of the associated linear conservative system. It is computed solving the following generalized eigenvalue problem:

$$(-\omega_i^2\mathbf{M}+\mathbf{K})\boldsymbol{\phi}_i=\mathbf{0}, \tag{7}$$

where ω_i is the i-th natural frequency and $\boldsymbol{\phi}_i$ is the i-th normal mode. Therefore, $\mathbf{\Phi}=[\boldsymbol{\phi}_1\ \boldsymbol{\phi}_2\ \boldsymbol{\phi}_3\ldots]$. This is the best basis for a linear dynamical system if the modes are chosen properly. However, the system under analysis is nonlinear due to the impacts. It should be noted that, in this case, the reduced matrices are diagonal: $\mathbf{M}_{rij}=\delta_{ij}$, $\mathbf{K}_{rij}=\delta_{ij}\omega_i^2$ and $\mathbf{C}_{rij}=\delta_{ij}\omega_i\xi_i$, where ξ_i is the i-th damping rate and δ_{ij} is the Kronecker delta (δ_{ij} is equal to one if $i=j$ and is equal to zero if $i\neq j$).

The second basis is the $\mathrm{POD_{dir}}$-basis, for which the elements are called proper orthogonal modes (POMs). In this case, the system response is modeled as a second-order stochastic process, with the assumptions that the process is stationary in time and ergodic [2,3]. The dimensions of the matrix of interest is $m\times m$, which is related to the spatial mesh. This basis should be used when measurements from experiments are available, since there will be few points in the spatial mesh.

The third basis is the $\mathrm{POD_{snap}}$-basis, which is similar to $\mathrm{POD_{dir}}$-basis. However, the construction is very different. The dimensions of the matrix of interest is $n_t\times n_t$, which is related to the temporal mesh. This basis should be used to analyze a fast phenomenon, since the dynamics will be well represented from the snapshots of few instants.

For details about the construction of $\mathrm{POD_{dir}}$-basis and $\mathrm{POD_{snap}}$-basis see [9,12].

4. Convergence criterion

The convergence analysis is made using the following norm in $\mathcal{H}^1(\Omega)$ (Sobolev space, where $\Omega=[0,L]$) [13]:

$$\|u(\cdot,t)\|=\sqrt{\int|u(x,t)|^2\,\mathrm{d}x+\int|u'(x,t)|^2\,\mathrm{d}x}, \tag{8}$$

where u' is the derivative with respect to x. As the number of elements N of the basis used in the approximation increases, the approximation $u^N(\cdot,t)$ approaches $u(\cdot,t)$. The approximation $u^N(\cdot,t)$ is obtained after interpolating $\mathbf{u}^N(t)$. As $u(\cdot,t)$ is not known, the error in the approximation is pursue using the following error measure:

$$e^N=\frac{100}{t_1-t_0}\int_{t_0}^{t_1}\left(\frac{\|\mathbf{u}^N(t)-\mathbf{u}^{N-1}(t)\|}{\|\mathbf{u}^N(t)\|}\right)\mathrm{d}t, \tag{9}$$

where $[t_0,t_1]$ is the duration analyzed, $\mathbf{u}^N(t)$ is the approximation of the response of the step N of the computation, and $\mathbf{u}^{N-1}(t)$ is the approximation of the previous step; N is related to the number of elements of the basis. The analysis is done fixing an error ε and searching for N, such that $e^N<\varepsilon$.

5. Numerical results

For the numerical analysis, it was used a bar with cross-sectional area $A=7.9\times10^{-3}\,\mathrm{m}^2$, length $L=1$ m, and gap$=0.1\times10^{-3}$ m. The bar is made of steel with elasticity modulus $E=210$ MPa, density $\rho=7850\,\mathrm{kg/m}^3$. The excitation parameters are $A_f=5000$ N and $\omega_f=260$ Hz. The obstacle stiffness is $k=1\times10^{11}$ N/m. The time integration was done using an explicit Runge–Kutta method of fourth and fifth orders with adaptive time-step and the duration was $t=[0;0.02]$. The computer used to run the simulation was a Pentium(R), 2 GB RAM and 3,2 GHz, 32 bits.

5.1. Influence of damping

An analysis of the influence of the damping in the dynamical response is done. Table 1 shows the values of the damping rates related to the first five normal modes of the system for different values of (α,β). If α or β is too big, there are some modes that are overdamped ($\xi>1$). See, for instance, the cases of $(\alpha=10^6,\beta=0)$ and $(\alpha=0,\beta=10^5)$.

Now we analyze the dynamics of the system, first for $(\alpha=10^4,\ \beta=0)$. Fig. 2(a) shows the displacement of the endpoint ($x=L$) and Fig. 2(b) shows how the impact force changes with time, where the dashed line represents the location of the

Table 1
Damping rates related to the first five normal modes of the system for different values of α and β.

	$\alpha=10^4$, $\beta=0$		$\alpha=10^6$, $\beta=0$
ξ_1	0.0102		1.0234
ξ_2	0.0034		0.3411
ξ_3	0.0020		0.2047
ξ_4	0.0015		0.1462
ξ_5	0.0011		0.1137
	$\alpha=0$, $\beta=10^4$	$\alpha=0$, $\beta=10^5$	$\alpha=10^5$, $\beta=10^4$
ξ_1	0.0252	0.2522	0.1276
ξ_2	0.0757	0.7567	0.1098
ξ_3	0.1261	1.2612	0.1466
ξ_4	0.1766	1.7657	0.1912
ξ_5	0.2270	2.2702	0.2384

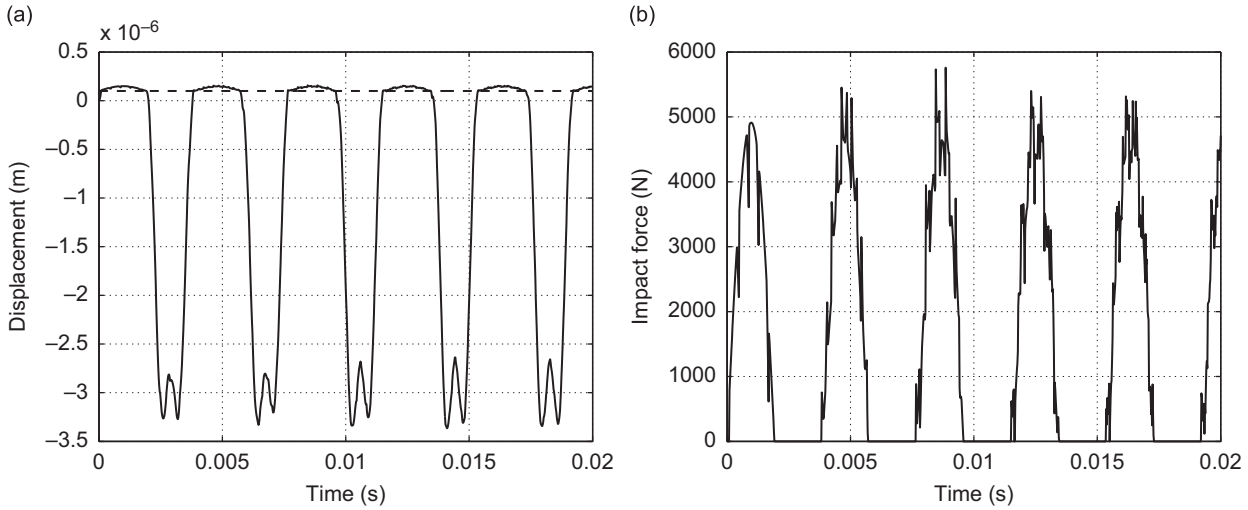

Fig. 2. (a) Displacement of the bar at $x=L$ as a function of time (the dashed line represents the obstacle locations), and (b) impact force as a function of time.

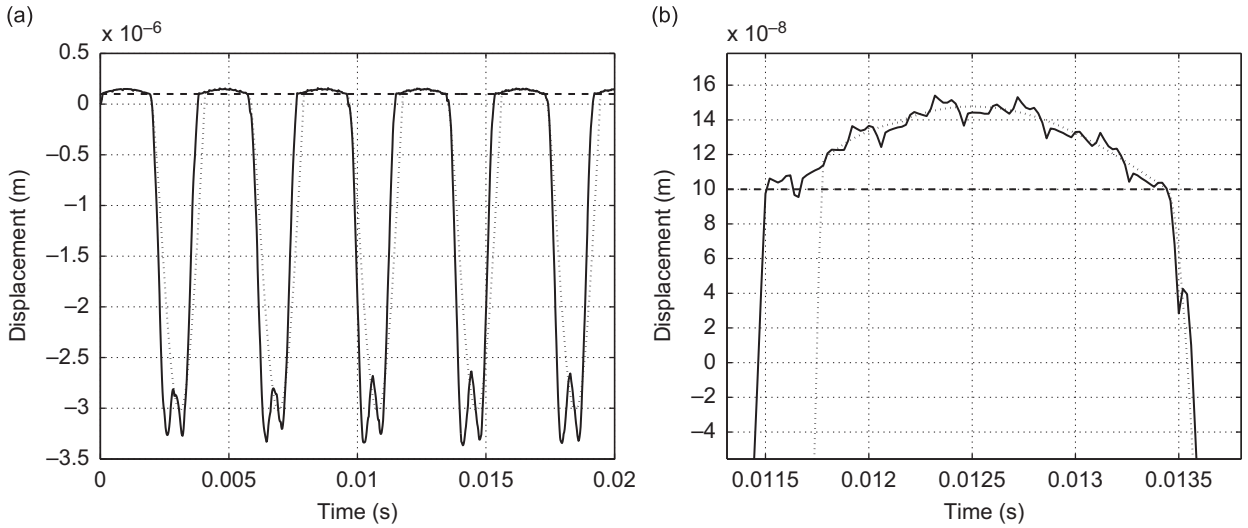

Fig. 3. (a) Displacement of the bar at $x=L$ as a function of time for two damping conditions: $\alpha=10^4$, $\beta=0$ (continuous line) and $\alpha=10^6$, $\beta=0$ (dotted line), and (b) detail of the impact region.

obstacle. When the bar hits the obstacle there is a reaction force (impact force) forcing the bar to move back. Of course, the impact force is zero when the bar does not touch the obstacle; see Fig. 2(b).

Fig. 3 shows the displacement of the endpoint (x=L) for different damping conditions: (1) ($\alpha=10^4,\beta=0$) and (2) ($\alpha=10^6,\beta=0$). Fig. 3(b) shows the same response in the impact region, where we can note less oscillations for the overdamped system ($\alpha=10^6$). As damping increases there are less oscillations of the structure, hence, the analysis is simplified in the sense that less elements of the reduced-order model will be able to capture the nonlinear dynamics in analysis. This is why the damping is kept small in the analysis of the next subsection; it is taken as ($\alpha=10^4,\beta=0$).

5.2. Comparing the different approximations

The convergence curves for the different models are shown in Fig. 4. The precision increases with the increasing of the number of elements; for illustration of the dimension of the reduced-order model, we fix the error as $\varepsilon=2$ percent. Using the finite element method (Fig. 4(a)), it is necessary 150 elements to represent the problem; using the LIN-basis (Fig. 4(b)), it is necessary 80 normal modes; using the POD_{dir}-basis (Fig. 4(c)), it is necessary 40 empirical modes; and using the POD_{snap}-basis (Fig. 4(d)), it is necessary 50 empirical modes. Beware that it does not mean that POD_{snap}-basis is always worse than POD_{dir}-basis. Comparing Fig. 4(c) with Fig. 4(d) one can notice that for an error of 1 percent it is necessary 50 empirical modes from both POD_{dir}-basis and POD_{snap}-basis. For the construction of the POD-basis, the response was computed for different force amplitudes A_f, and 1000 points were considered for both spatial and temporal meshes.

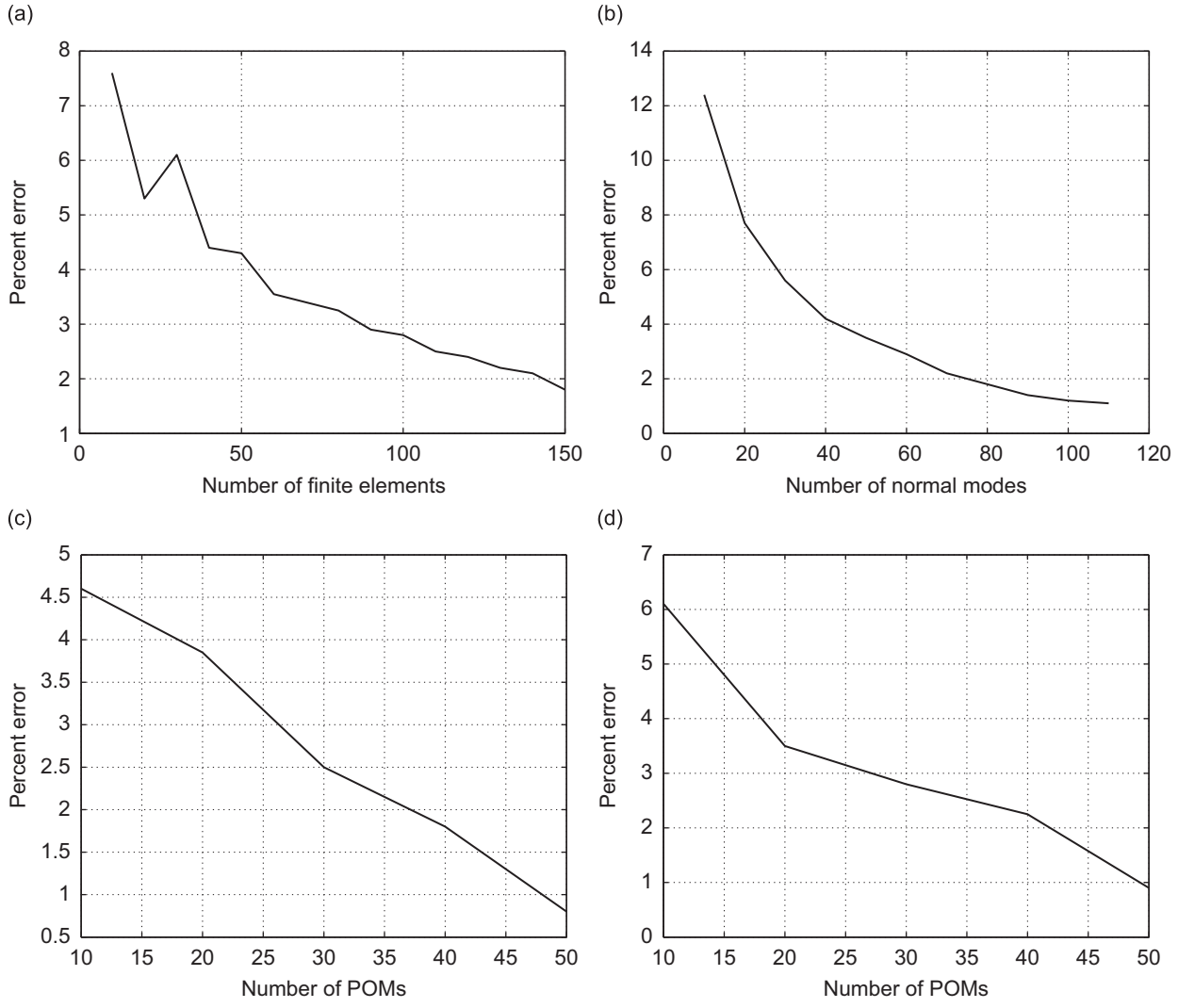

Fig. 4. Convergence for the different bases: (a) FEM, number of finite elements *versus* percent error, (b) LIN-basis, number of normal modes *versus* percent error, (c) POD-direct, number of POMs *versus* percent error, and (d) POD-snapshots, number of POMs *versus* percent error.

Up to this point, there is nothing new, the novelty comes now. Although POD-basis is the best basis in a certain sense (given a fixed number of elements, no other linear decomposition represents better the problem) it is not assured that the time-integration problem will be solved faster using the POD-basis. Fig. 5(a) shows that, for the problem analyzed, if the precision is fixed, POD-basis needs less elements to represent the problem. However, if the number of elements is fixed, POD-basis needs more time to compute the time response; see Fig. 5(b). Appendix A elucidates this point analyzing the condition number of the matrices used in the time-integration scheme.

Thus, one needs to check the efficiency of a basis to construct a reduced-order model taking into account the precision wanted and *also* the time required for the time-integration process; see Fig. 6. This figure shows that, for the problem in analysis, POD-basis is the most efficient one: besides making the greater reduction of the model, the time-integration process is faster, fixing the precision.

Fig. 7 shows a comparison between POD_{dir}-basis and POD_{snap}-basis. It shows that, for the problem in analysis, the basis constructed by the snapshots method is more complicated than the one constructed by the direct method. The time required for the time integration (for 50 POMs) is 28.6 min using the POD_{snap}-basis, and it is 15.9 min using POD_{dir}-basis. In Figs. 5 and 6, POD-basis refers to POD_{dir}-basis.

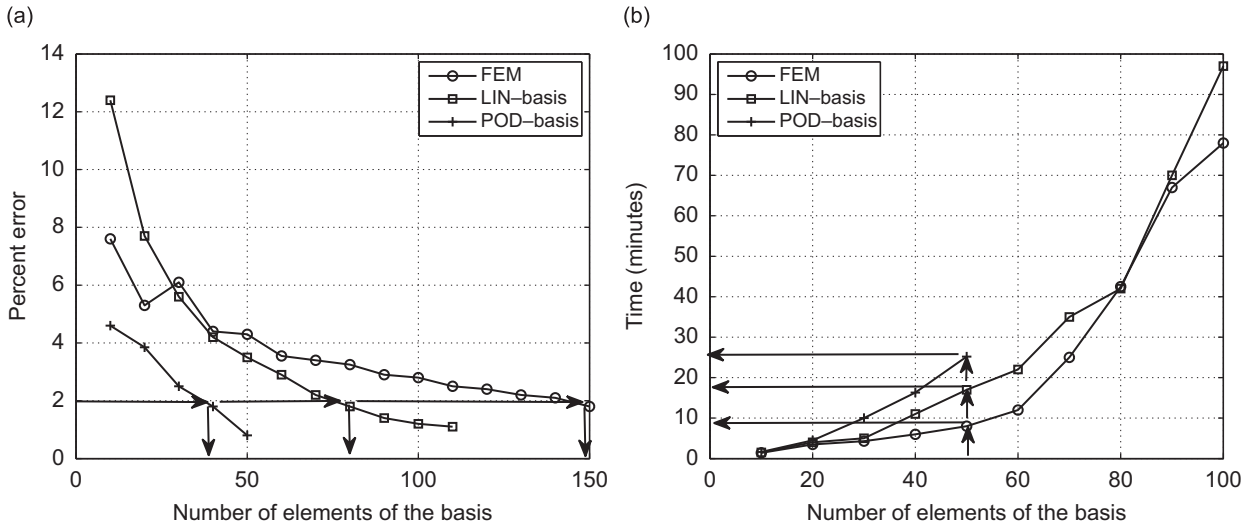

Fig. 5. (a) Convergence: number of elements of the basis *versus* percent error. (b) Number of elements of the basis *versus* time (minutes) spent in the numerical integration. –o– FEM, –□– LIN-basis and –+– POD-basis.

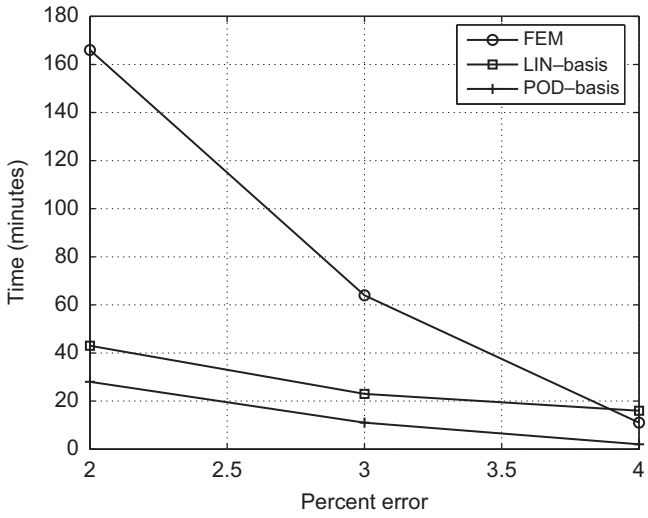

Fig. 6. Percent error *versus* time (minutes) required for the time-integration process. –o– FEM, –□– LIN-basis and –+– POD-basis.

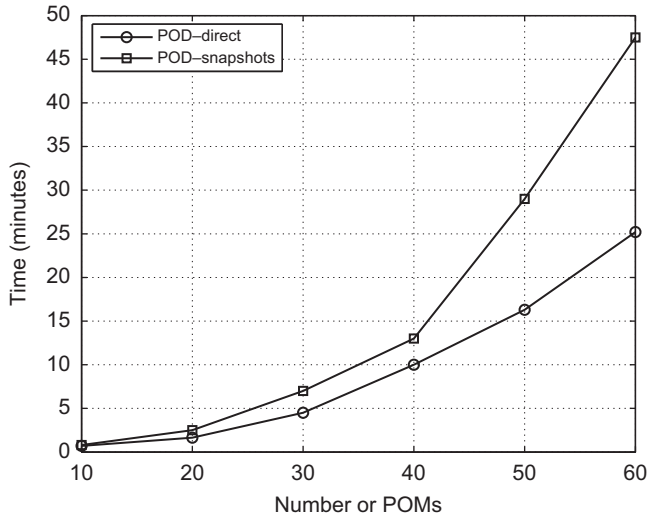

Fig. 7. Number of elements of the basis *versus* time (minutes) spent in the numerical integration. –o– POD-direct, –□– POD-snapshots.

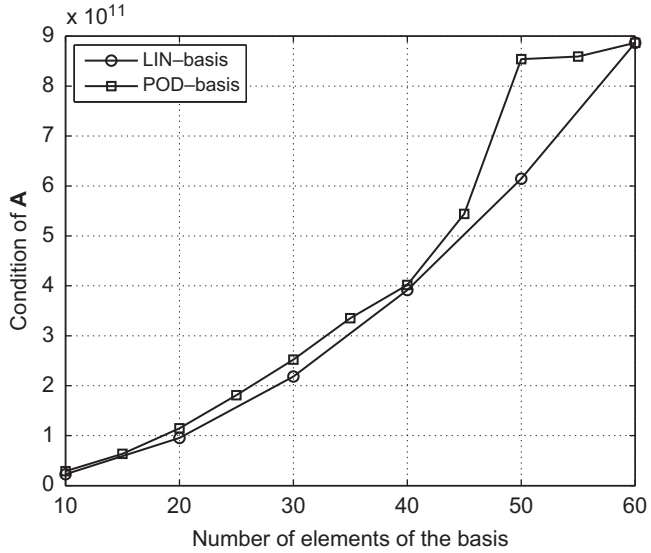

Fig. A1. Number of elements of the basis *versus* condition number of matrix **A**. –o– LIN-basis, –□– POD-basis.

6. Conclusions

A new way to measure the efficiency between LIN-basis and POD-basis to construct a reduced-order model in Structural Dynamics has been proposed. One should take into account the precision wanted and also the time required for the time-integration simulation (see Fig. 6). A vibroimpact system has been used to show this new idea. For the problem analyzed, POD-basis has performed better than LIN-basis in the sense that (1) the size of the resulting reduced matrices are smaller (fixing the precision), and (2) the time required for the time-integration simulation is lower (fixing the precision).

Acknowledgments

The authors gratefully acknowledge the support of the Brazilian agencies CNPQ, FAPERJ and CAPES, and the Argentinean agencies CONICET and SGCyT.

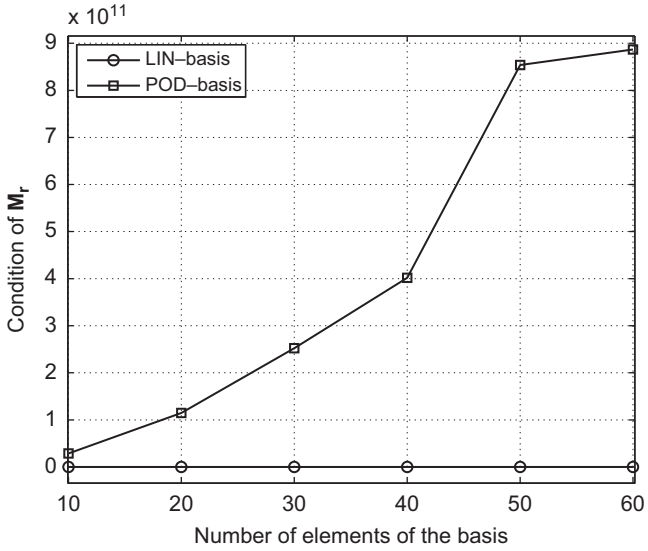

Fig. A2. Number of elements of the basis *versus* condition number of matrix $\mathbf{M}_r$. –o– LIN-basis, –□– POD-basis.

Appendix A. Condition number

The time-integration scheme might be written as

$$\begin{bmatrix} \dot{\mathbf{q}} \\ \ddot{\mathbf{q}} \end{bmatrix}^{(t+1)} = \underbrace{\begin{bmatrix} \mathbf{0} & \mathbf{I} \\ -\mathbf{M}_r^{-1}\mathbf{K}_r & -\mathbf{M}_r^{-1}\mathbf{C}_r \end{bmatrix}}_{\mathbf{A}} \begin{bmatrix} \mathbf{q} \\ \dot{\mathbf{q}} \end{bmatrix}^{(t)} + \begin{bmatrix} \mathbf{0} \\ \mathbf{M}_r^{-1}\boldsymbol{\Phi}^{\mathrm{T}}(\mathbf{f}+\mathbf{f}_{\mathrm{imp}}(\boldsymbol{\Phi}\mathbf{q})) \end{bmatrix}^{(t)}, \tag{10}$$

where $\mathbf{0}$ is the zero matrix and $\mathbf{I}$ is the identity matrix. The condition number of $\mathbf{A}$ is higher for POD-basis, compared to LIN-basis; see Fig. A1.

Note that if the system has geometric nonlinearity (e.g., $\mathbf{K}_r(\mathbf{q})$), matrix $\mathbf{A}(\mathbf{q})$ should be computed for each instant. For this reason and also to better compare the differences between LIN-basis and POD-basis, the algorithm is implemented in a way that $\mathbf{A}$ is computed at each time step. Doing so, the effect of a bad condition matrix is amplified in the analysis; meaning that it takes more time to do the time integration. It should be noticed that POD-basis has performed better than LIN-basis for the problem analyzed, even considering this bad scenario where $\mathbf{A}$ is computed at each time step.

Fig. A2 shows that the condition number of $\mathbf{M}_r$ increases when the POD-basis is used, while the condition number of $\mathbf{M}_r$ is always equal to one (identity matrix) when LIN-basis is used.

References

[1] M. Loève, *Probability Theory. Graduate Texts in Mathematics*, fourth ed., Springer, USA, 1977.
[2] P. Holmes, J.L. Lumley, G. Berkooz, *Turbulence, Coherent Structures, Dynamical Systems and Symmetry*, Cambridge University Press, Cambridge, 1996.
[3] S. Bellizzi, R. Sampaio, POMs analysis of randomly vibrating systems obtained from Karhunen-Loève expansion, *Journal of Sound and Vibration* 297 (3–5) (2006) 774–793.
[4] S. Bellizzi, R. Sampaio, Smooth Karhunen–Loève decomposition to analyze randomly vibrating systems, *Journal of Sound and Vibration* 23 (4) (2009) 1218–1222.
[5] P. Glusmann, E. Kreuzer, On the application of Karhunen–Loève transform to transient dynamic systems, *Journal of Sound and Vibration* 328 (4–5) (2009) 507–519.
[6] A.R. Khattak, S. Garvey, A. Popov, Proper orthogonal decomposition of the dynamics in bolted joints, *Journal of Sound and Vibration* 329 (9) (2010) 1480–1498.
[7] M. Meyer, H.G. Matthies, Efficient model reduction in non-linear dynamics using the Karhunen–Loève expansion and dual-weighted-residual methods, *Computational Mechanics* 31 (2003) 179–191.
[8] R. Sampaio, C. Soize, Remarks on the efficiency of POD for model reduction in non-linear dynamics of continuous elastic systems, *International Journal for Numerical Methods in Engineering* 72 (1) (2007) 22–45.
[9] M.F.A. Azeez, A.F. Vakakis, Proper orthogonal decomposition (POD) of a class of vibroimpact oscillation, *Journal of Sound and Vibration* 240 (5) (2001) 859–889.
[10] M.A. Trindade, C. Wolter, R. Sampaio, Karhunen–Loève decomposition of coupled axial/bending vibrations of beams subjected to impact, *Journal of Sound and Vibration* 279 (2005) 1015–1036.
[11] K.J. Bathe, *Finite Element Procedures*, Prentice-Hall Inc., USA, 1996.
[12] C. Wolter, M.A. Trindade, R. Sampaio, Obtaining mode shapes through the Karhunen–Loève expansion for distributed-parameter linear systems, *Shock and Vibration* 9 (4–5) (2002) 177–192.
[13] E. Kreyszig, *Introductory Functional Analysis with Applications*, first ed., Wiley, USA, 1989.